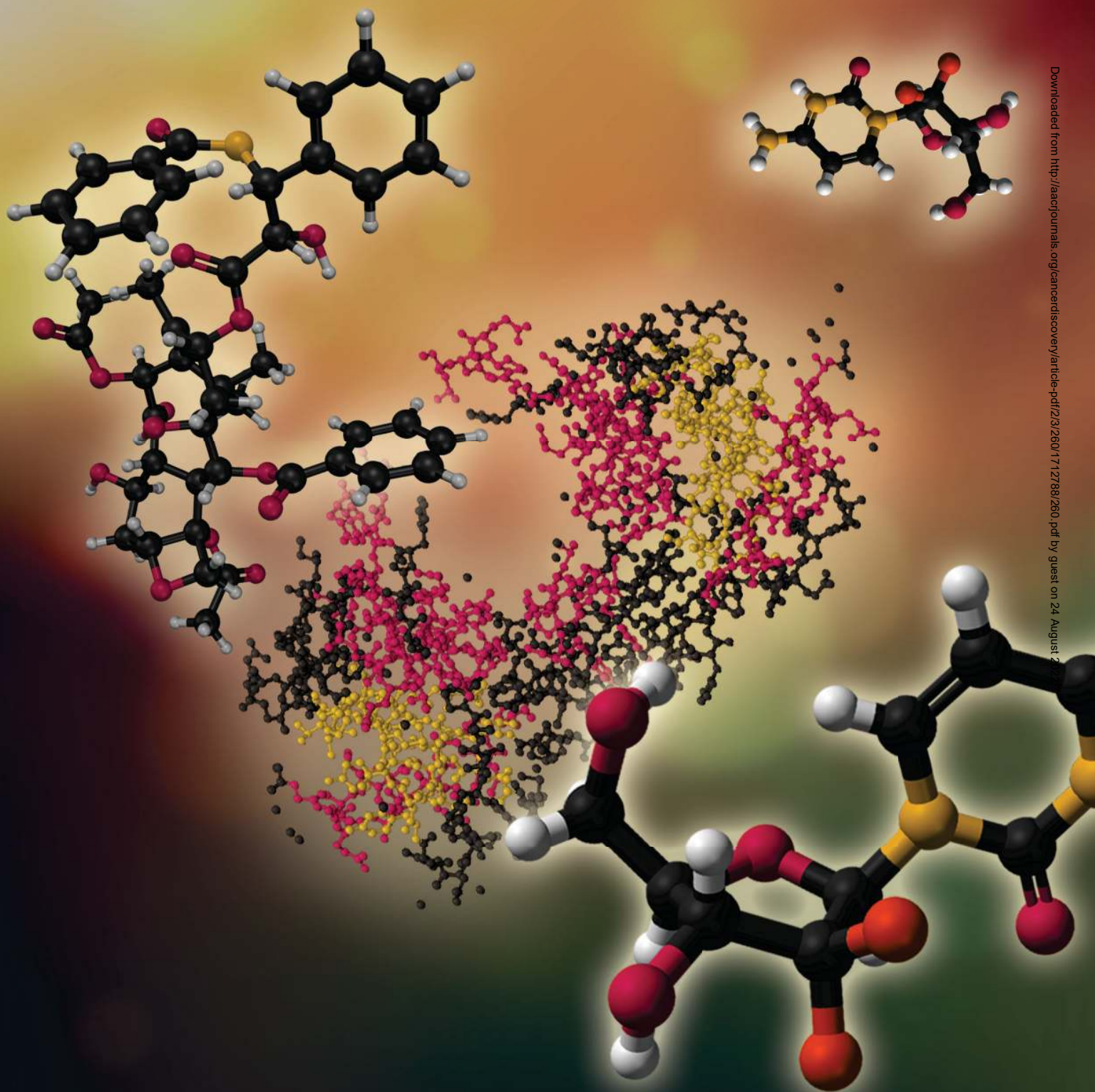nab-Paclitaxel Potentiates Gemcitabine Activity by Reducing Cytidine Deaminase Levels in a Mouse Model of Pancreatic Cancer

Kristopher K. Frese [1], Albrecht Neesse[1,3], Natalie Cook[1,2], Tashinga E. Bapiro[1,2], Martijn P. Lolkema[1,4], Duncan I. Jodrell[1,2], and David A. Tuveson[1,2]

ABSTRACT

Nanoparticle albumin-bound (*nab*)-paclitaxel, an albumin-stabilized paclitaxel formulation, demonstrates clinical activity when administered in combination with gemcitabine in patients with metastatic pancreatic ductal adenocarcinoma (PDA). The limited availability of patient tissue and exquisite sensitivity of xenografts to chemotherapeutics have limited our ability to address the mechanistic basis of this treatment regimen. Here, we used a mouse model of PDA to show that the coadministration of *nab*-paclitaxel and gemcitabine uniquely demonstrates evidence of tumor regression. Combination treatment increases intratumoral gemcitabine levels attributable to a marked decrease in the primary gemcitabine metabolizing enzyme, cytidine deaminase. Correspondingly, paclitaxel reduced the levels of cytidine deaminase protein in cultured cells through reactive oxygen species–mediated degradation, resulting in the increased stabilization of gemcitabine. Our findings support the concept that suboptimal intratumoral concentrations of gemcitabine represent a crucial mechanism of therapeutic resistance in PDA and highlight the advantages of genetically engineered mouse models in preclinical therapeutic trials.

SIGNIFICANCE: This study provides mechanistic insight into the clinical cooperation observed between gemcitabine and *nab*-paclitaxel in the treatment of pancreatic cancer. *Cancer Discovery; 2(3); 260–9.* ©2012 AACR.

INTRODUCTION

Pancreatic ductal adenocarcinoma (PDA) remains one of the most aggressive tumors in humans. A striking clinical feature of PDA is its innate resistance to available chemotherapies, resulting in a 5-year survival rate of less than 5%. The standard systemic chemotherapy for PDA is gemcitabine, but treatment with gemcitabine only marginally extends a patient's survival, and combinations with a second cytotoxic agent have so far proved largely ineffective (1, 2). Recent data in mice and humans suggest that poor drug delivery attributable to highly desmoplastic and hypovascular tumors and rapid metabolic inactivation of therapeutic agents may be at least partly responsible for this unusually poor response to treatment (3, 4).

Therefore, methods that can increase intratumoral gemcitabine levels in PDA are under active investigation. Recently, it was proposed that nanoparticle albumin-bound (*nab*)-paclitaxel, a water-soluble albumin-bound formulation of paclitaxel, could disrupt the

PDA stromal architecture in tumor xenografts and induce reactive angiogenesis, resulting in increased perfusion and delivery of gemcitabine (5). *nab*-Paclitaxel initially was developed to avoid toxicities associated with oil-based solvents required to solubilize paclitaxel, such as Cremophor EL (BASF Corp; ref. 6). Preclinical and clinical data have demonstrated superior efficacy and safety of *nab*-paclitaxel over solvent-based paclitaxel (7, 8), thus leading to approval by the U.S. Food and Drug Administration in 2005 as a second-line therapy for the treatment of patients with metastatic breast cancer.

The mechanism of delivery of *nab*-paclitaxel has been proposed to be mediated by active transport of albumin into the interstitial space via gp60-mediated transcytosis (9). In addition, secreted protein, acidic and rich in cysteine (SPARC), also known as osteonectin, is highly expressed and secreted by PDA peritumoral fibroblasts (10) and may serve as an albumin-binding protein that sequesters *nab*-paclitaxel to concentrate the drug intratumorally. Elevated expression of SPARC has been correlated with improved response to *nab*-paclitaxel; however, this effect may be tumor-type specific (5, 11, 12). Given that PDA is a stromal-rich tumor with abundant SPARC expression, in a series of clinical trials investigators are evaluating the combination of *nab*-paclitaxel and gemcitabine in patients with metastatic PDA. Initial results from a phase I/II trial in stage IV pancreatic cancer patients recently were reported; they demonstrated promising clinical activity in patients with PDA (5). More recently, an international phase III trial was initiated for patients with metastatic pancreatic cancer who were randomized to gemcitabine or gemcitabine plus *nab*-paclitaxel (13).

In clinical trials, the investigation of mechanisms of actions of novel drug combinations is often hampered by the paucity of available tumor tissue for detailed pharmacologic, biochemical, and histologic analysis. Genetically engineered mouse models (GEMM) constitute a promising platform for

Authors' Affiliations: [1]Cambridge Research Institute, Li Ka Shing Centre, and [2]Department of Oncology, University of Cambridge, Cambridge, United Kingdom; [3]Department of Gastroenterology, Endocrinology and Metabolism, Philipps University Marburg, Baldingerstr, Marburg, Germany; and [4]Department of Medical Oncology, University Medical Center Utrecht, Utrecht, The Netherlands

K. K. Frese and A. Neesse contributed equally to this article.

Corresponding Author: David A. Tuveson, Cancer Research UK, Cambridge Research Institute, the Li Ka Shing Centre, Robinson Way, Cambridge CB2 0RE, UK. Phone: 44-1223-404306; Fax: 44-1223-404199; E-mail: david.tuveson@cancer.org.uk

A

|	Non-tumor (n = 12)	UnTx (n = 16)	Vehicles (n = 12)	Gem (n = 16)	nP (n = 14)	nP + Gem (n = 14)
8-day survival	NA	ND	58%	56%	50%	71%
Metastasis incidence	NA	ND	92%	88%	86%	76%
Ascites	NA	ND	44%	36%	0%	27%
WBC (10^6 cells/mL)	2.7 ± 0.3	21.1 ± 6.7	19.4 ± 5.1	23.4 ± 9.2	11.0 ± 2.8	82 ± 16
Neutrophils (10^6 cells/mL)	0.11 ± 0.02	2.71 ± 1.40	4.88 ± 2.10	3.46 ± 1.42	3.39 ± 1.00	2.38 ± 0.54
Platelets (10^6 cells/mL)	516 ± 51	493 ± 112	510 ± 120	413 ± 73	394 ± 56	354 ± 56
Hgb (g/dL)	13.1 ± 1.0	7.5 ± 0.9	7.5 ± 1.1	9.4 ± 1.3	9.9 ± 0.9	9.7 ± 0.9
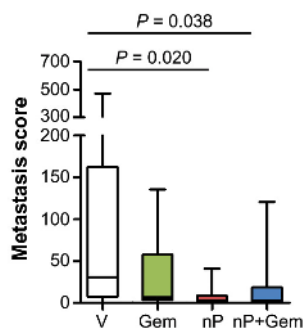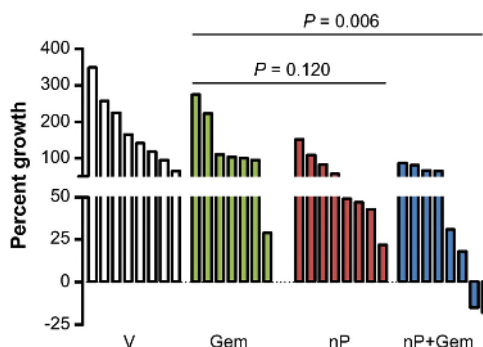
Figure 1. *nab*-Paclitaxel (nP) slows tumor growth, improves survival, and decreases metastasis. **A,** the percentage of mice who survived for 8 days, exhibited at least one metastasis, or developed ascites was quantified. Analysis of terminal blood draws was used to measure white blood cell count (WBC), neutrophil/granulocyte count, platelet count, and hemoglobin (Hgb). Normal ranges for healthy littermate non–tumor-bearing mice as well as untreated KPC mice are listed. Gem, gemcitabine; NA, not applicable; ND, not determined; UnTx, untreated. **B,** liver metastasis score was quantified by factoring the number and size of metastases throughout the liver. Please see Methods for additional information (n ≥ 9). **C,** waterfall plot of tumor response of individual tumors from each cohort. *nab*-Paclitaxel (nP) monotherapy was significantly better than vehicle (V) but not gemcitabine (P = 0.006 and P = 0.120, respectively).

preclinical testing of novel drugs because many GEMMs recapitulate the molecular and clinical features of the cognate human malignancy (14, 15). Because tumor tissue can be readily obtained at predefined time points, GEMMs enable the direct correlation between drug levels, response to treatment, and alterations at the cellular and molecular level. Thus, the potential efficacy of drug combinations and also mechanisms of resistance can be identified, guiding the selection and rapid translation of more effective therapies for human cancers.

We have previously described a GEMM of PDA that is based upon the pancreatic specific expression of endogenous mutant *Kras* and *Trp53* alleles (16). Such mutant mice, termed KPC mice (LSL-Kras^{G12D}; LSL-Trp53^{R172H}; Pdx-1-Cre), develop primary pancreatic tumors that faithfully recapitulate the clinical, histopathologic, pharmacokinetic, and molecular features of the human disease (17). Furthermore, unlike many transplantation models of PDA, KPC mice demonstrate innate resistance to gemcitabine (3). Here, we investigated the antitumor efficacy and the molecular mechanism of action of *nab*-paclitaxel and gemcitabine in KPC mice.

RESULTS

Combination of *nab*-Paclitaxel and Gemcitabine Causes Tumor Regression and Reduces Metastasis

To test the efficacy of *nab*-paclitaxel in the KPC model, we treated mice with established tumors of comparable size for 8 days with vehicle, gemcitabine, *nab*-paclitaxel, or *nab*-paclitaxel/gemcitabine (Supplementary Fig. S1A and B). Consistent with clinical reports (18, 19), both *nab*-paclitaxel monotherapy and *nab*-paclitaxel/gemcitabine treatments were well tolerated, with blood counts found to be in acceptable ranges (Fig. 1A and Supplementary Fig. S1C). Mice treated with combination therapy were more likely to survive the entire treatment regimen (Fig. 1A). Furthermore, combination treatment modestly reduced metastasis incidence, and quantification of liver metastases revealed a significant decrease in metastatic burden in both the *nab*-paclitaxel cohort and the *nab*-paclitaxel/gemcitabine cohort when it was compared with the vehicle cohort (Fig. 1A and B).
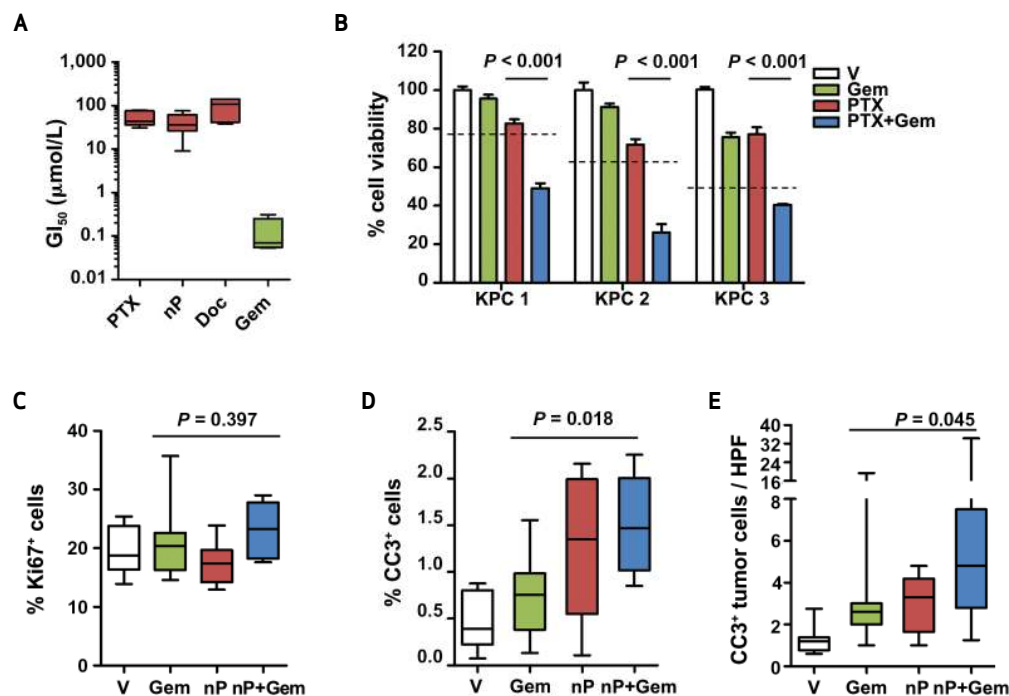
Figure 2. *nab*-Paclitaxel targets the tumor epithelial cells. **A,** KPC cell lines (*n* = 8) were exposed to a dose range of paclitaxel (PTX), *nab*-paclitaxel (nP), docetaxel (Doc), or gemcitabine (Gem) for 3 days to determine the concentration needed to reduce the growth of treated cells to half that of untreated cells (GI_{50}) of each agent. Data are representative of 4 independent experiments. **B,** KPC cell lines (*n* = 3) were exposed to sub-GI_{50} levels of agents. Cells were pretreated with dimethyl sulfoxide or 10 μmol/L paclitaxel for 24 hours and/or treated with 30 nmol/L gemcitabine for 2 days. Data are representative of 2 independent experiments. The dotted lines represent predicted additive effect of combination therapy. Proliferation (**C**) and apoptosis (**D**) in tumors were measured via quantitative immunohistochemistry for Ki67^{+} and cleaved caspase 3 (CC3^{+}), respectively (*n* = 8). **E,** 10–20 high-powered fields (HPF) per tumor were quantified by performing coimmunofluorescence for cleaved caspase 3 (CC3^{+}) and E-cadherin (*n* ≥ 9).

Consistent with clinical observations, gemcitabine treatment alone had no statistically significant effect on tumor growth. Tumors in mice treated with single–agent *nab*-paclitaxel (mean, 170% ± 15%) did not significantly differ from the gemcitabine cohort (*P* = 0.12). Treatment with *nab*-paclitaxel/gemcitabine resulted in significantly smaller tumors (mean, 140% ± 15%) as compared with gemcitabine (mean, 234% ± 32%; *P* < 0.01) and vehicle (mean, 278% ± 33%; Supplementary Fig. S1D). Importantly, 2 tumors in the *nab*-paclitaxel/gemcitabine cohort regressed after only 8 days of treatment (Fig. 1C). Because *nab*-paclitaxel is formulated with human serum albumin, we were unable to treat mice continuously to assess longer-term survival benefit because of the development of a mouse anti-human albumin humoral immune response (Supplementary Fig. S1E).

nab-Paclitaxel Treatment Targets Tumor Epithelial Cells

Gemcitabine and paclitaxel are chemotherapeutic agents that have been shown to elicit their antitumoral effects through induction of apoptosis or a cell-cycle arrest in G_1 or G_2–M, respectively. Although KPC cells display similar sensitivity to paclitaxel and *nab*-paclitaxel *in vitro*, the elevated maximum tolerated dose *in vivo* permitted increased intratumoral paclitaxel levels in the *nab*-paclitaxel–treated cohort (Fig. 2A and Supplementary Fig. S2A). *In vitro*, cells derived from KPC tumors are much more sensitive to gemcitabine

than taxanes, and pretreatment with paclitaxel sensitizes cells to gemcitabine (Fig. 2A and B). Similarly, treatment with both drugs yielded a significant increase in apoptosis in tumors treated with *nab*-paclitaxel/gemcitabine compared with gemcitabine alone, whereas there were no significant changes in proliferation (Fig. 2C and D). This finding correlated with the appearance of aberrant mitotic figures that contained an abundance of phosphorylated histone H3 (Supplementary Fig. S2B and C). Necrotic areas were present in the majority of tumors but did not significantly differ among the treatment groups (Supplementary Fig. S2D).

Contrary to the observation that *nab*-paclitaxel promotes stromal disruption in a human xenograft model (5), histologic assessment did not reveal any evidence for changes in stromal content or composition (Supplementary Fig. S2E). The vast majority of apoptotic cells were E-cadherin-expressing neoplastic cells rather than α-smooth muscle actin (α-SMA)–expressing stromal cells, and these apoptotic cells were significantly increased only in *nab*-paclitaxel/gemcitabine–treated mice (Fig. 2E and Supplementary Fig. S2F). Moreover, neither intratumoral α-SMA content nor collagen density significantly changed upon treatment with *nab*-paclitaxel (Supplementary Fig. S3A–D). In support of the lack of effect upon stromal cells in KPC tumors, SPARC levels remained unchanged upon treatment (Supplementary Fig. S3E–F). Therefore, we concluded that the antitumor effect
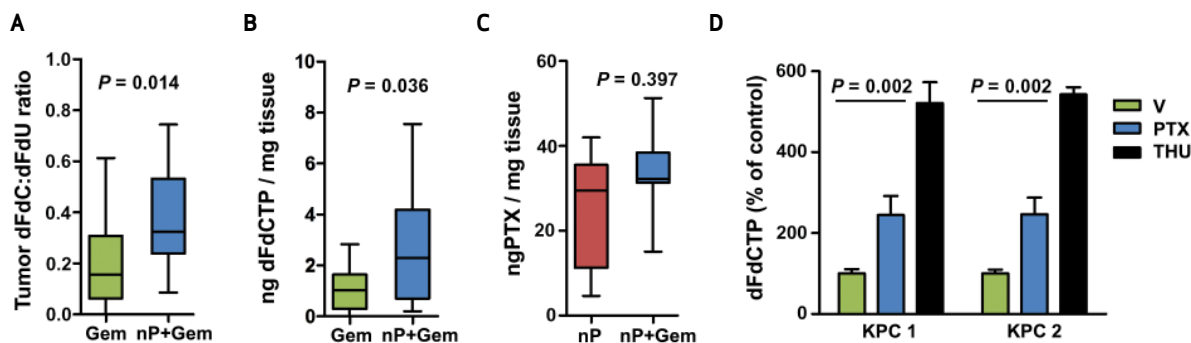
Figure 3. *nab*-Paclitaxel promotes elevated intratumoral gemcitabine levels. **A,** 2′,2′-difluorodeoxcytidine:2′,2′-difluorodeoxyuridine (dfdC:dFdU) ratio in bulk tumor was quantified in mice 2 hours after the last dose of gemcitabine. ($n \geq 12$). **B,** intratumoral levels of dFdCTP were measured in duplicate samples from mice in each cohort 2 hours after the last dose of gemcitabine. ($n \geq 12$) **C,** intratumoral levels of paclitaxel were measured in samples from mice in each cohort 4 hours after the last dose of *nab*-paclitaxel ($n \geq 7$). **D,** 2 KPC cell lines were pretreated with 10 μmol/L paclitaxel or dimethyl sulfoxide for 36 hours or 10 μmol/L tetrahydrouridine (THU; cytidine deaminase inhibitor) for 30 minutes as a positive control and incubated with 1 μmol/L gemcitabine for 2 hours. Levels of dFdCTP were then measured. Data are representative of 3 independent experiments. G, gemcitabine; nP + G, *nab*-paclitaxel and gemcitabine.

of *nab*-paclitaxel, in particular in combination with gemcitabine, is mediated by induction of apoptosis in tumor cells rather than stromal cells.

nab-Paclitaxel Promotes Elevated Intratumoral Gemcitabine Levels

We have previously demonstrated that treatment with the hedgehog inhibitor IPI-926 promotes gemcitabine delivery, resulting in enhanced antitumor effects and a doubling of survival time (3). We therefore wanted to determine whether the enhanced antitumor activity of *nab*-paclitaxel/gemcitabine stemmed from increased drug delivery. By using a highly sensitive method, we examined the intratumoral levels of the gemcitabine prodrug 2′,2′-difluorodeoxycytidine (dFdC), as well as its inactivated and activated metabolites 2′,2′-difluorodeoxyuridine (dFdU) and gemcitabine triphosphate (dFdCTP), respectively (20). Notably, we found that combination treatment with *nab*-paclitaxel elevated the dFdC:dFdU ratio and increased the amount of dFdCTP in tumors (Fig. 3A and B, Supplementary Table S1).

Conversely, paclitaxel concentrations were not significantly different between the *nab*-paclitaxel/gemcitabine group and the single-agent *nab*-paclitaxel cohort, suggesting that overall drug delivery was not affected (Fig. 3C). Unlike treatment with IPI-926, treatment with *nab*-paclitaxel did not affect vascular density or structure, as measured by microvascular density or mean vascular lumen area, respectively (Supplementary Fig. S4A and B). Finally, we found that the treatment of cultured PDA cells with free paclitaxel significantly elevated dFdCTP levels, indicating that the chemotherapeutic component in *nab*-paclitaxel directly affects the metabolism of gemcitabine independent of any alterations in vascular delivery (Fig. 3D).

nab-Paclitaxel Decreases Cytidine Deaminase Protein Levels

To assess the mechanism of increased levels of dFdCTP in tumors, we performed real-time PCR on RNA extracted from

bulk tumor for a variety of enzymes involved in gemcitabine transport and metabolism. Among these, only 2 genes were significantly downregulated (*Ent2* and *Tk2*) and one gene was upregulated (*Cnt3*; Supplementary Fig. *S5A*); however, decreased expression of *Ent2* and *Tk2* would be predicted to decrease rather than enhance the formation of dFdCTP. The lack of commercially available antibodies against murine Cnt3 has prevented us from further investigating this gene; however, siRNA-mediated knockdown of Cnt3 had no effect on the sensitivity of tumor cells to gemcitabine (Supplementary Fig. S5B).

Conversely, knocking down Ent1, an established gemcitabine transporter, decreased sensitivity to gemcitabine, whereas depletion of Cda, the primary gemcitabine catabolic enzyme, increased sensitivity to gemcitabine (Supplementary Fig. S5B). A subset of proteins for which reliable antibodies were available was examined in bulk tumor cell lysates. Strikingly, protein levels of Cda were lower in both the *nab*-paclitaxel and gemcitabine/*nab*-paclitaxel cohorts, whereas expression of deoxycytidine kinase and equilibrative nucleoside transporter 2 remained unchanged (Fig. 4A). Immunohistochemical analysis revealed that Cda is primarily expressed in the tumor epithelial cells and that treatment with *nab*-paclitaxel decreased its expression (Fig. 4B).

To determine whether this phenotype was attributable to a direct effect on tumor cells or indirectly mediated through the microenvironment, we assessed the effects of paclitaxel on cultured KPC tumor cells *in vitro*. Whereas the mRNA levels of *Cda* were not altered by treatment with free paclitaxel in culture, protein levels were substantially reduced, indicating that paclitaxel can act directly on tumor cells (Fig. 4C and D). Treatment of cells with the proteasome inhibitor MG132 reversed the effects of paclitaxel on Cda, indicating that paclitaxel regulates Cda protein stability through a posttranslational mechanism (Fig. 4E).

Paclitaxel treatment generates reactive oxygen species (ROS) that result in a more oxidized intracellular environment that can be reverted with the free radical scavenger *N*-acetylcysteine (NAC; Fig. 5A and B). Considering the relative abundance of cysteine residues in Cda and the finding that 2 of these cysteines are highly reactive (21), we determined whether paclitaxel-induced
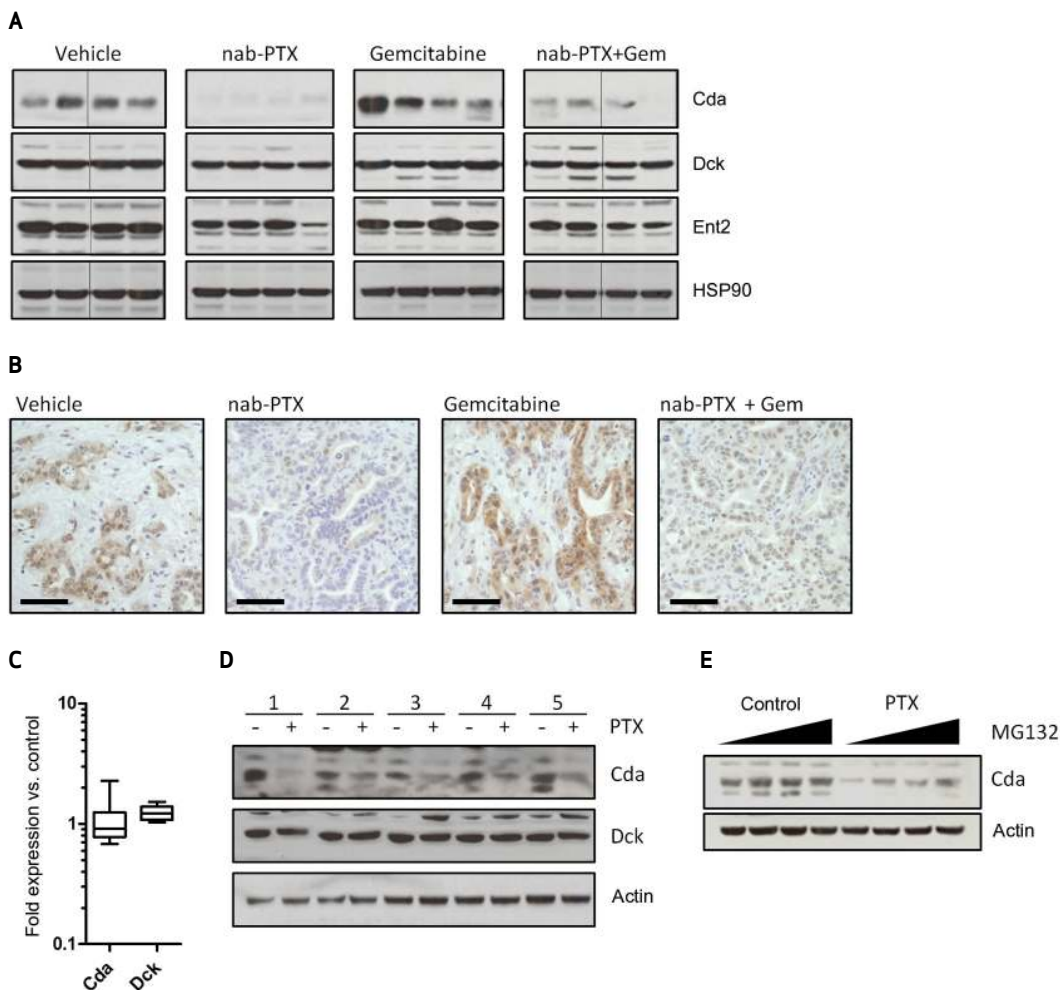
Figure 4. *nab*-Paclitaxel (nP) and paclitaxel (PTX) destabilize cytidine deaminase protein. **A,** 40 μg of bulk tumor cell lysates were immunoblotted for indicated proteins. **B,** immunohistochemistry for cytidine deaminase revealed reduced protein levels in tumor epithelial cells. Scale bar = 50 μm (*n* = 8). **C,** RNA isolated from 5 KPC cell lines treated for 36 hours with 10 μmol/L paclitaxel was subjected to quantitative reverse transcription PCR and revealed no alterations in mRNA levels compared with controls. Relative quantity values were generated using actin as an endogenous control. **D,** protein lysates were generated from the same 5 KPC cell lines treated for 36 hours with DMSO or 10 μmol/L paclitaxel and immunoblotted for indicated proteins. Data are representative of 4 independent experiments. **E,** protein lysates were generated from KPC cells pretreated for 36 hours with dimethyl sulfoxide or 10 μmol/L paclitaxel followed by 10 μmol/L MG132 for 0, 3, 10, or 30 minutes. Dck, deoxycytidine kinase; Ent2, equilibrative nucleoside transporter 2.

ROS had an effect on Cda. The paclitaxel-mediated decrease in Cda protein correlated with the induction of the antioxidant gene heme oxygenase (Fig. 5C). Conversely, treatment with NAC prevented the reduction in Cda protein levels. Importantly, NAC also inhibited the paclitaxel-mediated increase in dFdCTP, indicating that ROS is required for the effect of paclitaxel on gemcitabine activation (Fig. 5D). This observation was not restricted to paclitaxel because cisplatin, but not gefitinib, also reduced Cda levels, induced ROS, and elevated dFdCTP levels in cultured pancreatic cancer cells (Supplementary Fig. S6).

DISCUSSION

Although gemcitabine exhibits potent cytotoxicity against PDA cells *in vitro*, its short half-life may contribute to its relatively weak antitumor activity *in vivo*. Indeed, methods that increase gemcitabine delivery (3) or stability

(22) have been proposed to circumvent this problem clinically. Taxanes are also active in pancreatic cancer xenografts and patients, although treatment is limited by systemic toxicity (23, 24). *nab*-Paclitaxel is a solvent-free formulation composed of paclitaxel and human albumin with a mean particle size of 130 nm. It offers several advantages over solvent-based paclitaxel, including increased water solubility that obviates Cremophor EL-based toxicities. In addition, albumin is hypothesized to target paclitaxel to stromal-rich tumors and thereby increase the local concentration. Although combinations of gemcitabine and taxanes have demonstrated antitumor activity in patients with PDA, its toxicity has limited its use in the clinic (25). Accumulating clinical data support the combination of *nab*-paclitaxel and gemcitabine as an active regimen for patients with PDA; therefore, understanding the mechanisms of sensitivity will be necessary to prevent eventual therapeutic relapse.
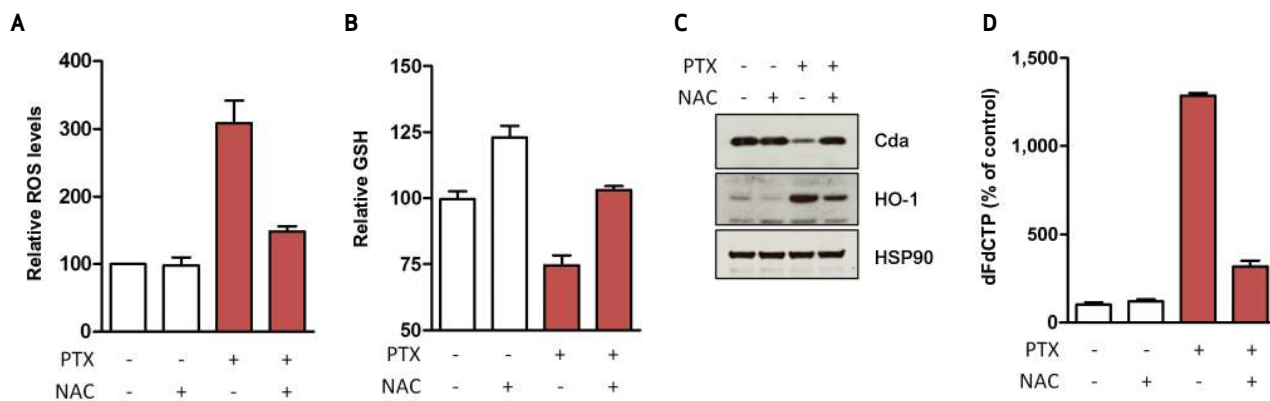
Figure 5. Paclitaxel inactivates cytidine deaminase through induction of ROS. KPC cells were pretreated with 10 μmol/L paclitaxel (PTX) and/or 5 mmol/L NAC for 4 hours and (**A**) incubated with CM-H2DCFDA to assess intracellular ROS via flow cytometry (*n* = 3) or (**B**) assessed for intracellular redox state via glutathione (GSH)-Glo (*n* = 3). **C,** protein lysates were generated from KPC cells treated for 36 hours with 10 μmol/L paclitaxel (PTX) and/or 5 mmol/L NAC and immunoblotted for indicated proteins. **D,** KPC cells were pretreated with 10 μmol/L paclitaxel (PTX) and/or 5 mmol/L NAC for 36 hours and incubated with 1 μmol/L gemcitabine for 1 hour. Intracellular dFdCTP was measured (*n* = 3).

A recently published phase I/II clinical trial for stage IV patients demonstrated that the addition of *nab*-paclitaxel to gemcitabine has tolerable adverse effects and robust antitumor activity (5). Although the study was not designed to assess clinical efficacy, the median survival achieved with *nab*-paclitaxel/gemcitabine (12.2 months) is comparable with results for FOLFIRINOX [5-fluorouracil, leucovorin, irinotecan, and oxaliplatin (11.1 months)] and substantially better than gemcitabine monotherapy (6.8 months) in a phase III trial with comparable patients (26). Our results indicate that *nab*-paclitaxel/gemcitabine treatment effectively prevents tumor growth and uniquely causes tumor regression in some mice. Conversely, tumors treated with gemcitabine more than doubled in size during this time period. Although *nab*-paclitaxel monotherapy elicits some antitumor activity, it fails to cause any tumor regression in the KPC model. Together, these data suggest that *nab*-paclitaxel/gemcitabine combination therapy offers great potential for future use in the treatment of advanced pancreatic cancer.

Concurrent with our data, work with a xenograft model of PDA has shown that combination treatment with *nab*-paclitaxel and gemcitabine exhibits synergistic antitumor activity and improved drug delivery (5). Increased drug delivery was hypothesized to stem from stromal depletion and subsequent reactive angiogenesis through a mechanism similar to what has been described for IPI-926 (3). Conversely, we failed to demonstrate any measurable effect on the tumor stroma of KPC mice. One possible explanation for these disparate results may be the different dosing regimens. Although we gave the maximum tolerated dose, Von Hoff and colleagues (5) administered *nab*-paclitaxel as a low-dose metronomic therapy. Furthermore, stromal depletion occurred after 28 days of treatment, a time frame we could not assess because of the development of an acquired immune response to the human albumin component of *nab*-paclitaxel after 8 days of treatment. Another key difference is our use of a genetically engineered model that develops autochthonous tumors instead of a subcutaneous transplantation model in which human tumor cells must interact with murine stromal cells in

an immune-compromised mouse. This aberrant microenvironment may create conditions that render the stroma more sensitive to chemotherapeutic treatment.

Although our study did not reveal stromal depletion, both studies concluded that treatment with *nab*-paclitaxel elevates intratumoral gemcitabine levels. Interestingly, paclitaxel has previously been shown to alter gemcitabine pharmacokinetics in both plasma samples and non–small cell lung cancer cell lines (27–29); however, the mechanism of action was not determined. Here, we reveal that *nab*-paclitaxel treatment decreased protein levels of cytidine deaminase. Native gemcitabine, dFdC, is deaminated into the metabolite dFdU, which accounts for approximately 80% of the administered dose, with only 5% of native gemcitabine excreted unchanged in the urine within the first 6 hours (30, 31). Cda is ubiquitously expressed in mice and humans and can inactivate dFdC into dFdU in both plasma and cells (32, 33). Notably, recent *in vitro* and *in vivo* data have provided the first evidence that high Cda expression is associated with gemcitabine resistance, and a small study in pancreatic cancer patients showed that Cda ultrametabolizers were 5 times more likely to progress after gemcitabine-based therapy (30, 34, 35). Conversely, functionally deficient Cda has been associated with an increased risk of experiencing severe or even lethal adverse effects in patients (36, 37).

In our model, we found Cda protein levels, but not RNA levels, to be decreased upon treatment with *nab*-paclitaxel paralleled by a significant increase in dFdCTP and improved therapeutic efficacy. *In vivo*, Cda was primarily expressed by tumor cells, and the addition of paclitaxel to various KPC tumor cell lines consistently reduced Cda protein levels. Interestingly, the molecular mechanism for Cda degradation is mediated by paclitaxel-induced ROS. Upon ROS induction, Cda destabilizes and ultimately results in increased levels of active cytotoxic dFdCTP, an effect that is reversed by the ROS scavenger NAC. Although we found that other chemotherapeutic agents, such as cisplatin, are also capable of inducing ROS *in vitro*, the dramatically reduced toxicity profile of the *nab*-paclitaxel formulation allowed us to administer larger doses *in vivo* to execute the

synergistic effects on gemcitabine metabolism within the range of relatively mild side effects.

In conclusion, we have used a GEMM of pancreatic cancer to identify a mechanism for the synergistic antitumor effects of the combination of *nab*-paclitaxel and gemcitabine. *nab*-paclitaxel exhibits monotherapeutic antineoplastic effects and simultaneously depresses Cda levels through induction of ROS to stabilize gemcitabine and thereby sensitize the PDA tumor to combination treatment. These data uncover novel insight into the antitumor activity of *nab*-paclitaxel and provide a distinct mechanism for improving gemcitabine delivery to pancreatic tumors that warrants further investigation in the clinical setting.

METHODS

Cell Culture

Cell lines were derived from our murine KPC tumors as previously described (16) and maintained in DMEM (41966029; Invitrogen) + 10% FBS (SH30070.03; HyClone). Protein lysates were obtained by the use of RIPA buffer with protease and phosphatase inhibitors (38). Tetrahydrouridine (Merck) was dissolved in PBS and used as a positive control for Cda inhibition. Paclitaxel (T7191; Sigma-Aldrich), docetaxel (01885; Sigma-Aldrich), MG132 (474790; Merck), and gefitinib (G-4408; LC Labs) were dissolved in dimethyl sulfoxide, whereas cisplatin (P4394; Sigma-Aldrich), NAC (A9165; Sigma-Aldrich), and gemcitabine (Addenbrookes) were dissolved in saline and used as indicated. Cell viability experiments were performed via Cell Titer-Glo (G7570; Promega) or MultiTox-Glo Multiplex Cytotoxicity Assays (G9270; Promega) according to the manufacturer's recommended protocols. Intracellular GSH levels were measured via GSH Glo (V6911; Promega) according to the manufacturer's recommended protocols.

Mouse Strains

The KPC mice have been described previously (16). KPC mice develop advanced and metastatic pancreatic ductal adenocarcinoma with 100% penetrance at an early age, recapitulating the full spectrum of histopathologic and clinical features of human PDA. Mice were housed at a 12-hour light/12-hour dark cycle. All procedures were conducted in accordance to the institutional and national guidelines.

Quantitative PCR

Pancreatic tissue samples were immediately placed in an RNA later solution (QIAGEN) and stored for at least 24 hours at 4°C and then snap-frozen until they were processed. Total RNA was isolated by use of the QIAGEN TissueLyser and QIAGEN RNeasy kit. cDNA was synthesized from 1 µg of RNA using the Applied Biosystems QPCR cDNA Synthesis Kit (Applied Biosystems) and analyzed by quantitative real-time PCR on a 7900HT Real-Time PCR system using relative quantification ($\Delta\Delta$Ct) with the Taqman gene expression assays (Applied Biosystems). FAM-labeled assays are listed in the Supplementary Methods.

Western Blot Analysis

Western blots were performed as previously described (38). The following primary antibodies were used: heat shock protein 90, or Hsp90 (4874; Cell Signaling), phospho-ERK1/2 (4370; Cell Signaling), phospho-EGFR (4407; Cell Signaling), actin (I-19; Santa Cruz Biotechnology, Inc.), Cda (ab82346; Abcam), equilibrative nucleoside transporter 2 (ab48595; Abcam), and deoxycytidine kinase (ab96599; Abcam). Membranes were incubated with secondary horseradish peroxidase antibodies (Jackson ImmunoResearch) and developed by use of the ECL detection system (GE Healthcare).

Liquid Chromatography–Tandem Mass Spectrometry of Gemcitabine and Paclitaxel

dFdC, dFdU, and dFdCTP Fresh-frozen tumor samples and cell pellets were processed and analyzed on liquid chromatography–tandem mass spectrometry (LC-MS/MS) as previously described (20). To summarize in brief, LC-MS/MS was performed on a TSQ Vantage triple stage quadrupole mass spectrometer (Thermo Scientific) fitted with a heated electrospray ionization (HESI-II) probe operated in positive and negative mode at a spray voltage of 2.5 KV, capillary temperature of 150°C. Quantitative data acquisition was performed with LC Quan2.5.6 (Thermo Fisher Scientific).

Paclitaxel Fresh-frozen tumor samples were processed and analyzed for paclitaxel concentrations with the use of LC-MS/MS. To summarize in brief, samples were extracted with 90:10 acetonitrile/methanol, and LC-MS/MS was performed on a SCIEX API 4000TM mass spectrometer (Applied Biosystems/MDS SCIEX). Deuterated paclitaxel (d5-paclitaxel; Moravek) was used as the internal standard. Instrument control and quantitative data acquisition were performed by Analyst Version 1.42 (Applied Biosystems-MDS Sciex).

Histologic Examination

Tissues were fixed in 10% neutral buffered formalin for 24 hours and transferred to 70% ethanol. Tissues were embedded in paraffin, and 3- to 5-µm sections were processed for hematoxylin and eosin staining, immunohistochemistry, and immunofluorescence by the use of standard protocols as previously described (3). The following antibodies were used: SPARC (15274-1-AP; Proteintech), α-SMA (1A4; Dako), Cda (ab82346; Abcam), E-cadherin (612130; BD Pharmingen), Cleaved Caspase-3 (9661; Cell Signaling Technology), and CD31 (553370; BD Pharmingen). Images were acquired on an Olympus BX51 microscope or an Aperio XT automated scanning system and Imagescope 10 software (Aperio). More information can be found in Supplementary Methods.

ROS Quantification

ROS were quantified essentially as described (39). To summarize in brief, cells were treated as indicated and subsequently incubated with CM-H2DCFDA (C6827; Invitrogen) for 30 minutes in PBS, trypsinized, and analyzed via flow cytometry.

Statistical Analysis

Statistical analysis was performed with the use of GraphPad Prism version 5.01 (GraphPad Software). The Mann–Whitney nonparametric *t* test was used, and results are presented as mean $\pm$ SE. $P < 0.05$ was considered to be significant.

Disclosure of Potential Conflicts of Interest

No potential conflicts of interest were disclosed.

Author Contributions

Acknowledgments

REFERENCES

1. Burris HA 3rd, Moore MJ, Andersen J, Green MR, Rothenberg ML, Modiano MR, et al. Improvements in survival and clinical benefit with gemcitabine as first-line therapy for patients with advanced pancreas cancer: a randomized trial. J Clin Oncol 1997;15:2403–13.
2. Hidalgo M. Pancreatic cancer. N Engl J Med 2010;362:1605–17.
3. Olive KP, Jacobetz MA, Davidson CJ, Gopinathan A, McIntyre D, Honess D, et al. Inhibition of Hedgehog signaling enhances delivery of chemotherapy in a mouse model of pancreatic cancer. Science 2009;324:1457–61.
4. Komar G, Kauhanen S, Liukko K, Seppanen M, Kajander S, Ovaska J, et al. Decreased blood flow with increased metabolic activity: a novel sign of pancreatic tumor aggressiveness. Clin Cancer Res 2009;15:5511–7.
5. Von Hoff DD, Ramanathan RK, Borad MJ, Laheru DA, Smith LS, Wood TE, et al. Gemcitabine plus nab-paclitaxel is an active regimen in patients with advanced pancreatic cancer: a phase I/II trial. J Clin Oncol 2011;29:4548–54.
6. Gradishar WJ. Albumin-bound paclitaxel: a next-generation taxane. Exp Opin Pharmacother 2006;7:1041–53.
7. Desai N, Trieu V, Yao Z, Louie L, Ci S, Yang A, et al. Increased antitumor activity, intratumor paclitaxel concentrations, and endothelial cell transport of cremophor-free, albumin-bound paclitaxel, ABI-007, compared with cremophor-based paclitaxel. Clin Cancer Res 2006;12:1317–24.
8. Gradishar WJ, Tjulandin S, Davidson N, Shaw H, Desai N, Bhar P, et al. Phase III trial of nanoparticle albumin-bound paclitaxel compared with polyethylated castor oil-based paclitaxel in women with breast cancer. J Clin Oncol 2005;23:7794–803.
9. Vogel SM, Minshall RD, Pilipovic M, Tiruppathi C, Malik AB. Albumin uptake and transcytosis in endothelial cells in vivo induced by albumin-binding protein. Am J Physiol Lung Cell Mol Physiol 2001;281:L1512–22.
10. Infante JR, Matsubayashi H, Sato N, Tonascia J, Klein AP, Riall TA, et al. Peritumoral fibroblast SPARC expression and patient outcome with resectable pancreatic adenocarcinoma. J Clin Oncol 2007;25:319–25.
11. Desai N, Trieu V, Damascelli B, Soon-Shiong P. SPARC expression correlates with tumor response to albumin-bound paclitaxel in head and neck cancer patients. Transl Oncol 2009;2:59–64.
12. Shao H, Tang H, Salavaggione OE, Yu C, Hylander B, Tan W, et al. Improved response to nab-paclitaxel compared with cremophor-solubilized paclitaxel is independent of secreted protein acidic and rich in cysteine expression in non-small cell lung cancer. J Thorac Oncol 2011;6:998–1005.
13. National Institutes of Health. Phase III Study of ABI-007(Albumin-bound Paclitaxel) Plus Gemcitabine Versus Gemcitabine in Metastatic Adenocarcinoma of the Pancreas. ClinicalTrials.gov. Available from: clinicaltrials.gov/ct2/show/NCT00844649.
14. Becher OJ, Holland EC. Genetically engineered models have advantages over xenografts for preclinical studies. Cancer Res 2006;66:3355–8;discussion 8–9.
15. Frese KK, Tuveson DA. Maximizing mouse cancer models. Nat Rev Cancer 2007;7:645–58.
16. Hingorani SR, Wang L, Multani AS, Combs C, Deramaudt TB, Hruban RH, et al. Trp53R172H and KrasG12D cooperate to promote chromosomal instability and widely metastatic pancreatic ductal adenocarcinoma in mice. Cancer Cell 2005;7:469–83.
17. Hruban RH, Adsay NV, Albores-Saavedra J, Anver MR, Biankin AV, Boivin GP, et al. Pathology of genetically engineered mouse models of pancreatic exocrine cancer: consensus report and recommendations. Cancer Res 2006;66:95–106.
18. Roy V, LaPlant BR, Gross GG, Bane CL, Palmieri FM. Phase II trial of weekly nab (nanoparticle albumin-bound)-paclitaxel (nab-paclitaxel) (Abraxane) in combination with gemcitabine in patients with metastatic breast cancer (N0531). Ann Oncol 2009;20:449–53.
19. Stinchcombe TE, Socinski MA, Lee CB, Hayes DN, Moore DT, Goldberg RM, et al. Phase I trial of nanoparticle albumin-bound paclitaxel in combination with gemcitabine in patients with thoracic malignancies. J Thorac Oncol 2008;3:521–6.
20. Bapiro TE, Richards FM, Goldgraben MA, Olive KP, Madhu B, Frese KK, et al. A novel method for quantification of gemcitabine and its metabolites 2′,2′-difluorodeoxyuridine and gemcitabine triphosphate in tumour tissue by LC-MS/MS: comparison with (19)F NMR spectroscopy. Cancer Chemother Pharmacol 2011;68:1243–53.
21. Weerapana E, Wang C, Simon GM, Richter F, Khare S, Dillon MB, et al. Quantitative reactivity profiling predicts functional cysteines in proteomes. Nature 2010;468:790–5.
22. Beumer JH, Eiseman JL, Parise RA, Joseph E, Covey JM, Egorin MJ. Modulation of gemcitabine (2′,2′-difluoro-2′-deoxycytidine) pharmacokinetics, metabolism, and bioavailability in mice by 3,4,5,6-tetrahydrouridine. Clin Cancer Res 2008;14:3529–35.
23. Bissery MC, Guenard D, Gueritte-Voegelein F, Lavelle F. Experimental antitumor activity of taxotere (RP 56976, NSC 628503), a taxol analogue. Cancer Res 1991;51:4845–52.
24. Lenzi R, Yalcin S, Evans DB, Abbruzzese JL. Phase II study of docetaxel in patients with pancreatic cancer previously untreated with cytotoxic chemotherapy. Cancer Invest 2002;20:464–72.
25. Ryan DP, Kulke MH, Fuchs CS, Grossbard ML, Grossman SR, Morgan JA, et al. A Phase II study of gemcitabine and docetaxel in patients with metastatic pancreatic carcinoma. Cancer 2002;94:97–103.
26. Conroy T, Desseigne F, Ychou M, Bouche O, Guimbaud R, Becouarn Y, et al. FOLFIRINOX versus gemcitabine for metastatic pancreatic cancer. N Engl J Med 2011;364:1817–25.
27. Kroep JR, Giaccone G, Tolis C, Voorn DA, Loves WJ, Groeningen CJ, et al. Sequence dependent effect of paclitaxel on gemcitabine metabolism in relation to cell cycle and cytotoxicity in non-small-cell lung cancer cell lines. Br J Cancer 2000;83:1069–76.
28. Kroep JR, Giaccone G, Voorn DA, Smit EF, Beijnen JH, Rosing H, et al. Gemcitabine and paclitaxel: pharmacokinetic and pharmacodynamic interactions in patients with non-small-cell lung cancer. J Clin Oncol 1999;17:2190–7.
29. Shord SS, Faucette SR, Gillenwater HH, Pescatore SL, Hawke RL, Socinski MA, et al. Gemcitabine pharmacokinetics and interaction with paclitaxel in patients with advanced non-small-cell lung cancer. Cancer Chemother Pharmacol 2003;51:328–36.
30. Ciccolini J, Mercier C, Dahan L, Andre N. Integrating pharmacogenetics into gemcitabine dosing-time for a change? Nat Rev Clin Oncol 2011;8:439–44.
31. Abbruzzese JL, Grunewald R, Weeks EA, Gravel D, Adams T, Nowak B, et al. A phase I clinical, plasma, and cellular pharmacology study of gemcitabine. J Clin Oncol 1991;9:491–8.

32. Ruiz van Haperen VW, Veerman G, Boven E, Noordhuis P, Vermorken JB, Peters GJ. Schedule dependence of sensitivity to 2′,2′-difluorodeoxycytidine (gemcitabine) in relation to accumulation and retention of its triphosphate in solid tumour cell lines and solid tumours. Biochem Pharmacol 1994;48:1327–39.

33. Besnard T, Renee N, Etienne-Grimaldi MC, Francois E, Milano G. Optimized blood sampling with cytidine deaminase inhibitor for improved analysis of capecitabine metabolites. J Chromatogr B Analyt Technol Biomed Life Sci 2008;870:117–20.

34. Ogawa M, Hori H, Ohta T, Onozato K, Miyahara M, Komada Y. Sensitivity to gemcitabine and its metabolizing enzymes in neuroblastoma. Clin Cancer Res 2005;11:3485–93.

35. Yoshida T, Endo Y, Obata T, Kosugi Y, Sakamoto K, Sasaki T. Influence of cytidine deaminase on antitumor activity of 2′-deoxycytidine analogs in vitro and in vivo. Drug Metab Dispos 2010;38:1814–9.

36. Mercier C, Raynal C, Dahan L, Ortiz A, Evrard A, Dupuis C, et al. Toxic death case in a patient undergoing gemcitabine-based chemotherapy in relation with cytidine deaminase downregulation. Pharmacogenet Genomics 2007;17:841–4.

37. Ciccolini J, Dahan L, Andre N, Evrard A, Duluc M, Blesius A, et al. Cytidine deaminase residual activity in serum is a predictive marker of early severe toxicities in adults after gemcitabine-based chemotherapies. J Clin Oncol 2010;28:160–5.

38. Karreth FA, DeNicola GM, Winter SP, Tuveson DA. C-Raf inhibits MAPK activation and transformation by B-Raf(V600E). Mol Cell 2009;36:477–86.

39. DeNicola GM, Karreth FA, Humpton TJ, Gopinathan A, Wei C, Frese K, et al. Oncogene-induced Nrf2 transcription promotes ROS detoxification and tumorigenesis. Nature 2011;475:106–9.